

**Structure of thin SiO<sub>2</sub> films grown on Mo(112)**

M. S. Chen, A. K. Santra, and D. W. Goodman\*

*Department of Chemistry, Texas A&M University, P.O. Box 30012, College Station, Texas 77842-3012, USA*

(Received 11 November 2003; published 5 April 2004)

Ultra-thin SiO<sub>2</sub> films were prepared by evaporating Si onto a Mo(112) surface followed by oxidation and annealing up to 1200 K. The surface structure and film quality were investigated by low-energy electron diffraction (LEED), Auger spectroscopy (AES), and high-resolution electron energy loss spectroscopy (HREELS). A well-ordered, monolayer Mo(112)-*c*(2×2)-SiO<sub>2</sub> structure was characterized by HREELS and shown to exhibit unique phonon features compared to bulk SiO<sub>2</sub>. The phonon features are assigned to Si-O-Mo rather than Si-O-Si species, and the surface structure determined to be Mo(112)-*c*(2×2)-[SiO<sub>4</sub>] where each of the four oxygen atoms bonds to the substrate Mo atoms.

DOI: 10.1103/PhysRevB.69.155404

PACS number(s): 68.49.-h

**I. INTRODUCTION**

The growth of thin oxide films on refractory single-crystal metal surfaces as a means to circumvent problems associated with sample charging has received considerable attention during the last two decades.<sup>1–4</sup> In particular, SiO<sub>2</sub> single crystalline thin films, compared with bulk SiO<sub>2</sub> crystals, provide a convenient model of an important ceramic surface, and, indeed, are important in their own right with respect to tunnel junctions, catalyst supports, and corrosion barriers.<sup>4,5</sup> In addition, epitaxial  $\alpha$ -quartz films are important with respect to sensor technology,<sup>6,7</sup> light-emitting optical devices,<sup>8,9</sup> and imaging technologies.<sup>5</sup>

Numerous studies have focused on the preparation and characterization of thin oxide films; however, to date there are few reports of the growth of ordered crystalline SiO<sub>2</sub> films on metal surfaces: the growth of an 0.8 nm SiO<sub>2</sub> film on a Mo(112) surface<sup>10,11</sup> and a 4.0 nm SiO<sub>2</sub> film on a Ni(111) surface.<sup>12</sup> The growth recipe of SiO<sub>2</sub>/Mo(112) consists of repeated cycles of depositing one-half monolayer of silicon onto a Mo(112) surface at room temperature followed by oxidation at 800 K. The resulting SiO<sub>2</sub> films were subsequently annealed in two steps, one at 1000 K and a second at 1100 K. For SiO<sub>2</sub>/Ni(111), Si was deposited onto a clean Ni(111) surface at room temperature to a thickness of approximately 3 nm, followed by oxidation at 623 K in  $2 \times 10^{-7}$  Torr O<sub>2</sub> in an atomic hydrogen environment for 1 h, then finally annealed at 1073 K in  $2 \times 10^{-7}$  Torr O<sub>2</sub> for 10 min. Several studies in our laboratories have addressed the preparation and characterization of thin SiO<sub>2</sub> film on Mo(112)<sup>13–15</sup> particularly as model catalytic supports.<sup>16–19</sup>

In this paper, studies of the growth of thin SiO<sub>2</sub> films on a Mo(112) surface are described. Although a well ordered, monolayer SiO<sub>2</sub> film can be synthesized on the Mo(112) surface, SiO<sub>2</sub> films with thicknesses of 3–5 ML show little long-range order. Based on HREELS data and assessment of thickness by AES, the monolayer SiO<sub>2</sub> structure is found to be a Mo(112)-*c*(2×2)-[SiO<sub>4</sub>] complex where all four oxygen atoms bind directly to the substrate Mo atoms. This surface is very reproducible and stable in UHV, and therefore, is an excellent model for a catalytic support. Furthermore, by appropriately doping with dissimilar oxides, e.g., TiO<sub>x</sub>, this

SiO<sub>2</sub> film is an excellent model for a sinter-resistant support for metal particles. The structure of the isolated [SiO<sub>4</sub>] tetrahedron where all four oxygen atoms are bonded directly to the substrate is also relevant to sensor and specialty coatings technologies.

**II. EXPERIMENT**

The experiments were carried in an UHV chamber with a base pressure of  $3 \times 10^{-10}$  Torr and equipped with high-resolution electron energy loss spectroscopy (HREELS, LK-2000), low-energy electron diffraction (LEED), Auger electron spectroscopy (AES), and temperature programmed desorption (TPD). The AES data were acquired with a primary beam energy of 2000 eV. The energy resolution of the HREELS measurements was between 64 and 96 cm<sup>-1</sup> (8–12 meV); the monochromatized electrons were incident at an angle of 60° with respect to the surface normal of the sample. The analyzer could be rotated about its axis for on- and/or off-specular measurements; a primary energy (E<sub>p</sub>) of 5 eV was used.

The Mo(112) sample was cleaned by repeated cycles of oxidation at 1200 K followed by a flash to 2100–2200 K; cleanliness and order were verified with AES and LEED, respectively. Finally, the sample was flashed to 2100 K to remove any possible contaminant accumulation during surface analysis, then O<sub>2</sub> dosed at  $5 \times 10^{-8}$  Torr with the surface at 850 K for approximately 10 min. Following this procedure, a *p*(2×3)-O surface was obtained.<sup>13</sup> The substrate temperature was measured directly with a (W/5 wt % Re)/(W/26 wt % Re) thermocouple spot welded to the back sample surface. A liquid-nitrogen cryostat and an electron beam heater allowed control of the sample temperature between 90 and 2300 K.

The silica films were prepared by evaporating Si onto the Mo(112) surface from a tantalum filament in UHV at room temperature. Two annealing processes were carried out to obtain either thick or thin films, respectively. The first process consisted of depositing less than 1 ML Si onto a Mo(112)-*p*(2×3)-O surface, followed by annealing at 800 K in a  $1 \times 10^{-7}$  Torr O<sub>2</sub> for 5 min then increasing the temperature to 1200 K for an additional 5 min. This Si deposition and annealing were repeated several times until a con-

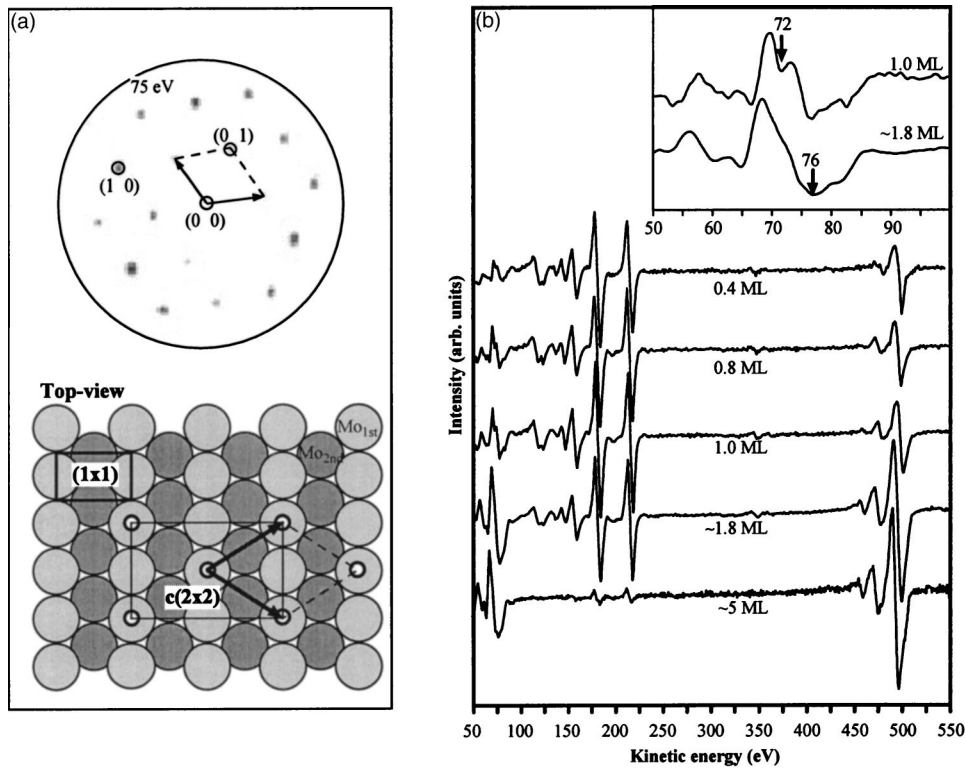


FIG. 1. (a) shows a  $c(2 \times 2)$  LEED pattern for monolayer  $\text{SiO}_2$  on  $\text{Mo}(112)$  along with a top view schematic of the clean  $\text{Mo}(112)$  surface. The dashed lines show the primitive reciprocal and real unit cell. (b) AES spectra of  $\text{SiO}_2$  films on  $\text{Mo}(112)$  with different  $\text{SiO}_2$  coverages.

stant Si/Mo AES ratio was achieved. The thickness was measured by AES to be approximately 1 ML (the details are discussed in the text); this coverage is referred to as 1 ML hereafter. This surface exhibits a sharp  $c(2 \times 2)$  LEED pattern [see Fig. 1(a) together with a top view of the  $\text{Mo}(112)$  surface], indicating a well-ordered surface structure. The second procedure (similar to that described in Ref. 11) consisted of depositing less than 0.5 ML Si onto an oxygen covered  $\text{Mo}(112)$  surface following by oxidation at 800 K in a  $5 \times 10^{-6}$  Torr  $\text{O}_2$  for 10 min. This cycle was repeated several times until the desired film thickness was obtained. The completed film was then annealed in  $5 \times 10^{-6}$  Torr in several steps, specifically, 1000, 1100, and 1200 K, each for 10 min. It is noteworthy that the first preparation recipe (Method I) leads to a film with a thickness not greater than 1 ML, while with the second recipe (Method II), a wide range of film thicknesses is possible. However, the thicker films shown in this paper generally lacked long-range order.

### III. RESULTS

The oxidation state of the synthesized films as indicated by AES are shown in Fig. 1(b). A comparison with Si and  $\text{SiO}_2$  standards shows an AES feature at 76 eV rather than one at 92 eV, consistent with stoichiometric  $\text{SiO}_2$  free of elemental Si, i.e., the Si is fully oxidized to  $\text{Si}^{4+}$ . Films with a thickness of 1 ML or less show a small peak at 72 eV that disappears as the films become thicker. This small peak arises possibly due to a particular silica structure with respect to the  $\text{Mo}(112)$  surface since the shape of the Si-LMM line is strongly influenced by the chemical environment.<sup>20</sup> The thickness  $d$  determined by the AES intensity attenuation of the Mo MNN (187 eV), is estimated to be 0.3 nm, i.e., one

layer of  $\text{SiO}_2$ , for films prepared by Method I. For the purpose of computing film thickness, a mean free path of 0.95 nm at 187 eV was used for  $\text{SiO}_2$ .<sup>21</sup>

Figure 2 shows the HREEL spectra acquired for each of the  $\text{SiO}_2$  films. For comparison, a spectrum of  $\text{SiO}_2(0001)$  is shown in the upper panel. The quartz spectrum is characterized by three features located at 498, 798, and  $1176 \text{ cm}^{-1}$ ,<sup>22</sup> corresponding to the bending, symmetric stretching, and asymmetric stretching modes of Si-O-Si.<sup>23</sup> The spectrum obtained from the film prepared by Method I [Fig. 2(a)] shows features at 320, 672, 768, and  $1048 \text{ cm}^{-1}$ . With an increase in the film thickness as indicated by the Si/Mo AES ratio [Figs. 1(a) and 1(b)], two additional features appear at 496 and  $1176 \text{ cm}^{-1}$  with a concomitant decrease in the intensities of the features at 672 and  $768 \text{ cm}^{-1}$ . With a further increase in the film thickness to approximately 5 ML of  $\text{SiO}_2$ , the  $1176 \text{ cm}^{-1}$  phonon peak becomes dominant [Fig. 2(d)]. This spectrum is very similar to that of  $\text{SiO}_2(0001)$  in Fig. 2 (upper panel), and therefore, is considered to be characteristic of the  $\text{SiO}_2$  film. It is noteworthy that the thicker film lacks long-range order as indicated by LEED, although the phonon structure is insensitive to the absence of this long-range order.<sup>22-24</sup> The thicker films were annealed to temperatures as high as 1250 K in an attempt to improve the long-range order, however, this led to a decrease in the film thickness and to an increase in the phonon structure corresponding to the monolayer film. Presumably this behavior is due to the partial decomposition of the film at the higher annealing temperatures.

Figure 3(a) shows HREEL spectra of Si coverages below 1 ML prepared by either Method I or II; the spectral features are characteristic of those exhibited by the 1 ML film. The

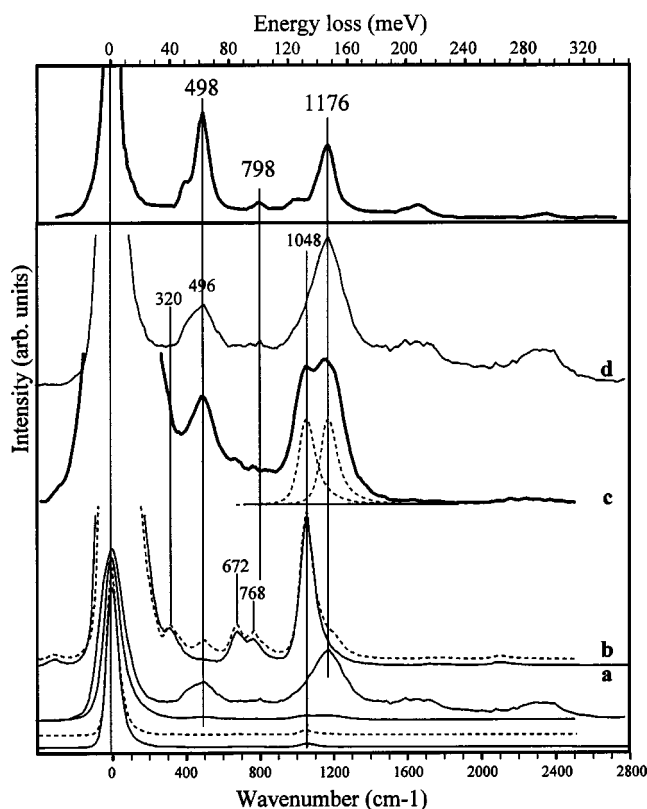


FIG. 2. (Upper panel) HREEL spectrum from quartz (0001) surface Ref. 22. (Lower panel) HREEL spectra of SiO<sub>2</sub> films at various coverages. (a) 1 ML, (b)  $\sim 1.2$  ML, (c)  $\sim 1.8$  ML, and (d)  $\sim 5$  ML.

main loss feature at  $1048\text{ cm}^{-1}$  corresponding to the Si-O asymmetric vibration mode does not shift, consistent with the local structures being essentially invariant with coverage. Figure 3(b) shows spectra of Si coverages higher than 1 ML prepared by Method II. All these spectra have a  $1048\text{ cm}^{-1}$  phonon feature with a shoulder at  $1176\text{ cm}^{-1}$  whose inten-

sity increases with an increase in the Si coverage. A well resolved feature at  $496\text{ cm}^{-1}$  appears concomitantly with the  $1176\text{ cm}^{-1}$  feature whose intensity increases with coverage. These results are consistent with there being two distinct Si-O species on the surfaces, one corresponding to the  $1048\text{ cm}^{-1}$  phonon feature and one to the  $496/1176\text{ cm}^{-1}$  phonon peaks.

#### IV. DISCUSSION

The monolayer SiO<sub>2</sub> film synthesized on Mo(112) by Method I described above exhibits unique surface phonon features that are distinctly different from those observed for thicker films made by Method II or measured for bulk SiO<sub>2</sub>.<sup>22–24</sup> In bulk SiO<sub>2</sub>, Si coordinates with four oxygen atoms to form a [SiO<sub>4</sub>] tetrahedron, where each of the four vertices is shared with a neighboring tetrahedron to form a continuous tetrahedral network. The structure of this monolayer including the precise orientation of the [SiO<sub>4</sub>] tetrahedron is a key to understanding whether such films can serve as useful surfaces for modeling terminated bulk silica. Therefore, the structure of this surface and the assignments of the surface phonon peaks are addressed in detail. First, we describe eight possible models of the arrangements of the [SiO<sub>4</sub>] tetrahedra in a  $c(2\times 2)$  periodicity. By assigning the HREELS phonon peaks, we then eliminate all but one of the eight possibilities.

It is appropriate to begin by discussing the possible arrangements of [SiO<sub>4</sub>] tetrahedra on the Mo(112) surface. It is noteworthy that this surface exhibits a sharp  $c(2\times 2)$  LEED pattern [cf. Fig. 1(a)] and that the thickness is estimated as a monolayer based on AES. Since AES indicates only the average thickness, there is a possibility of three-dimensional (3D) silica growth, however, this is highly unlikely because the film preparation involves repeated deposition of Si followed by annealing until a saturation coverage is obtained. Therefore, for a monolayer Mo(112)- $c(2$

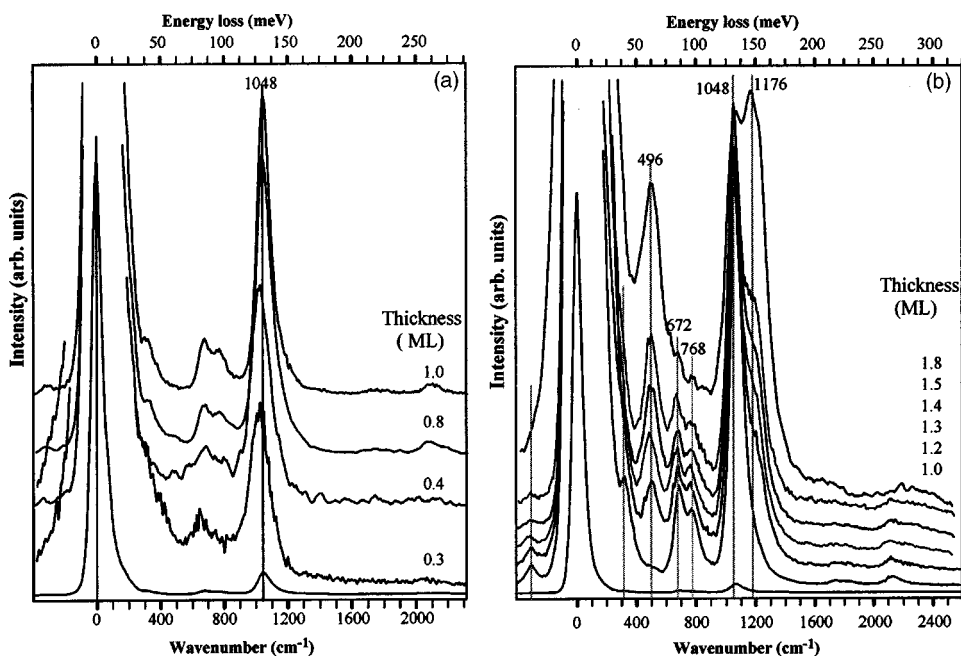


FIG. 3. HREEL spectra of various SiO<sub>2</sub> films at: (a) coverages lower than 1 ML; (b) coverages higher than 1 ML.



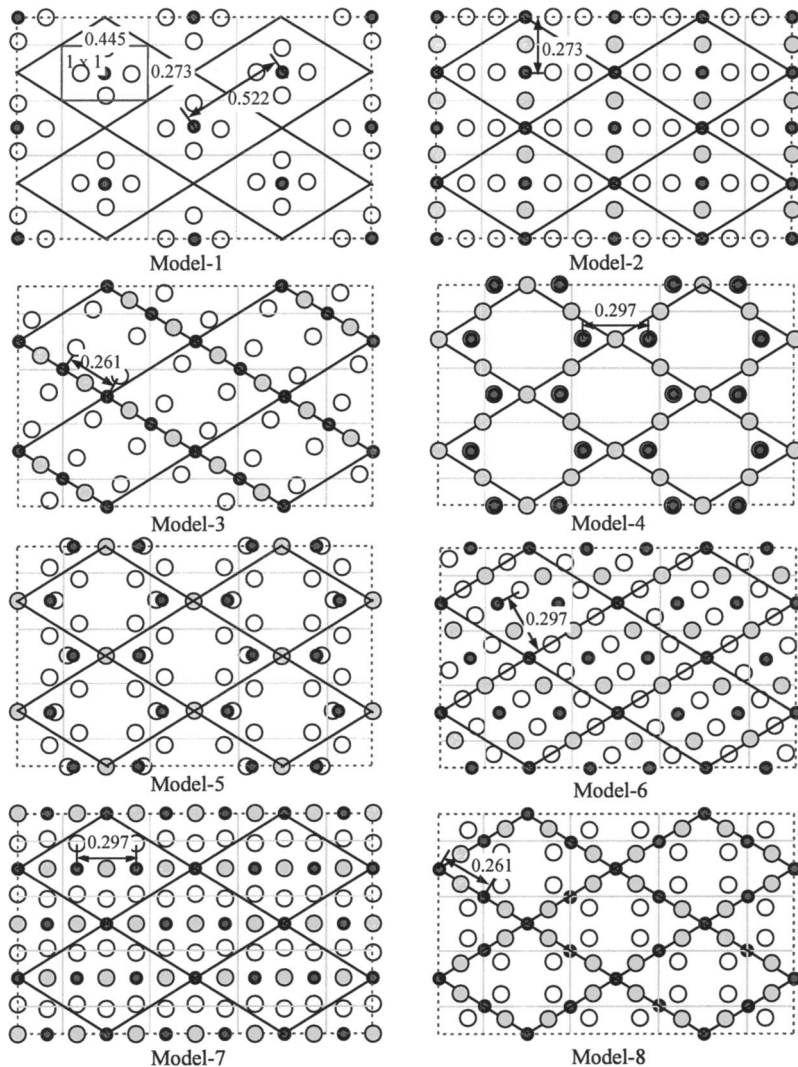


FIG. 4. Models for the possible arrangements of  $[\text{SiO}_4]$  tetrahedra on the Mo(112) surface. The black, cross-sectional lines show the Mo(112)- $c(2 \times 2)$  primitive unit, whereas the gray cross-sectional lines show the Mo(112)- $(1 \times 1)$  unit cell. The small black circles represent Si atoms, and larger white and dotted circles represent O atoms in Si-O-Mo and Si-O-Si bridges, respectively.

$\times 2$ )- $n$   $[\text{SiO}_4]$  surface structure, there can be 1, 2, or 3  $[\text{SiO}_4]$  tetrahedra per  $c(2 \times 2)$  unit cell. Four or more tetrahedra are not viable possibilities since in such structures the Si-Si distance is prohibitively close. The possible surface orientations of  $[\text{SiO}_4]$  tetrahedra are shown in Fig. 4. Models with dangling bonds or none bridging O atoms on Si are not considered viable possibilities since the surfaces prepared here are exceptionally unreactive to water or hydrocarbon impurities, consistent with fully saturated Si bonding.

Model 1 in Fig. 4 shows a single  $[\text{SiO}_4]$  tetrahedron in the  $c(2 \times 2)$  unit. In this model, each Si atom bonds with four oxygen atoms to form a tetrahedron where all four oxygen atoms bond to the substrate Mo atoms [see the schematic binding geometry in Fig. 5(a-1) and Fig. 5(b)], since in the  $c(2 \times 2)$  structure the lattice size (0.522 nm) is too large for two  $[\text{SiO}_4]$  tetrahedra to form a Si-O-Si bridge (the Si-Si distance in bulk  $\text{SiO}_2$  is 0.306–0.312 nm).<sup>25</sup>

Models 2–8 show the possible arrangements for two and three  $[\text{SiO}_4]$  tetrahedra in each  $c(2 \times 2)$  unit. Among them, models 2, 3, 6, and 7 form a chainlike structure in which each Si atom is incorporated into a  $[\text{SiO}_4]$  tetrahedron where two oxygen atoms bind to Mo atoms and another two oxygen atoms are shared with two neighboring  $[\text{SiO}_4]$  tetrahedra to

form bridging Si-O-Si bonds as illustrated in Fig. 5(a-2). This chainlike structure is similar to that of a relaxed quartz (0001) surface, where all the surface silicon atoms are four coordinated as Si-O-Si bridges, similar to the bulk quartz structure.<sup>26</sup> Model 4, the only 2D network possible for two Si atoms in a  $c(2 \times 2)$  unit, has one of the four oxygen atoms in the  $[\text{SiO}_4]$  tetrahedron bound to Mo atoms and the other three corner oxygen atoms shared with three neighboring Si atoms to form three Si-O-Si bridges [see Fig. 5(a-3)]. This model is similar to the structures of HP-tridymite and  $\beta$ -cristobalite (001) surfaces<sup>25</sup> that consist of sheets of corner sharing  $[\text{SiO}_4]$  tetrahedra joined in an hcp or fcc arrangement, respectively, where one corner oxygen of one tetrahedron is shared with the lower layer and every second tetrahedron shares an oxygen with the upper layer [see Fig. 5(a-4)]. Since there is only a single layer  $[\text{SiO}_4]$  tetrahedra on the Mo(112) surface, it is reasonable to assume that each  $[\text{SiO}_4]$  tetrahedra shares their one corner oxygen with the substrate Mo atoms [as shown in Fig. 4: model 4 and Fig. 5(a-3)]. Model 5 shows a dimer of two  $[\text{SiO}_4]$  tetrahedra sharing a corner oxygen in a  $c(2 \times 2)$  unit. (A dimer could share two corner oxygen atoms.) Model 8 is suggested by the structure of  $\beta$  quartz where one  $[\text{SiO}_4]$  tetrahedron shares its

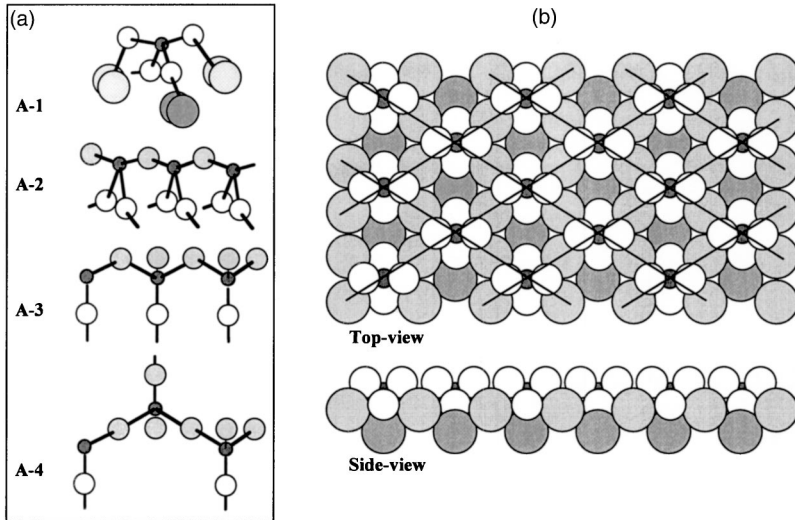


FIG. 5. (a) Schematic of  $[\text{SiO}_4]$  binding geometries for the models of Fig. 4: (a-1), isolated  $[\text{SiO}_4]$  binding with the substrate Mo atoms in model 1; (a-2), chain like structure for models 2, 3, 6, and 7; (a-3), two-dimension network for model 4; (a-4), two-dimension network for HP-tridymite and  $\beta$ -cristobalite (001) models. Small black circles, medium white, and dotted circles are Si, O in Si-O-Mo, and O in Si-O-Si bridging bonds, respectively. The large open circles are Mo atoms. (b) Top- and side-view of the possible structural model for  $\text{Mo(112)}-c(2 \times 2)-[\text{SiO}_4]$ . Black, white, and gray circles correspond to Si, O, and Mo atoms, respectively. The lines delineate the  $c(2 \times 2)$  primitive units.

four corner oxygen atoms with four neighboring  $[\text{SiO}_4]$  tetrahedra. Such coordination is likely energetically unfavorable since all  $[\text{SiO}_4]$  tetrahedra lie within the same layer in a single layer  $[\text{SiO}_4]$  structure. Note that in the chainlike structures (Models 2, 3, 6, and 7), the  $[\text{SiO}_4]$  tetrahedra can be arranged in a zig-zag pattern to increase the Si-O-Si bond angle to approximately  $145^\circ$ , the angle in bulk  $\text{SiO}_2$ .

The assignments of the surface phonon peaks observed for various thicknesses of  $\text{SiO}_2$  films on Mo(112) are now addressed. For a thicker film [Fig. 2(d)], the phonon peak shapes and positions ( $496$ ,  $800$ , and  $1176 \text{ cm}^{-1}$ ) are essentially the same as those measured for a quartz (0001) surface (Fig. 2, upper panel).<sup>22</sup> Accordingly,<sup>23</sup> these features are assigned to bending, symmetric stretching, and asymmetric stretching modes of Si-O-Si. However, for a single  $\text{SiO}_2$  layer [Fig. 2(a)], the phonon peaks at  $496$  and  $1176 \text{ cm}^{-1}$  are replaced by features at  $320$  and  $1048 \text{ cm}^{-1}$ . Increasing the film thickness to  $1$ – $2$  ML [Figs. 2(b) and 2(c), Fig. 3(b)], features at  $496$  and  $1176 \text{ cm}^{-1}$  appear (first as a shoulder peak at the high loss energy side of the  $1048 \text{ cm}^{-1}$  phonon peak) and increase in intensity with increasing film thickness. Note that the  $320 \text{ cm}^{-1}$  phonon peak is not well resolved from the elastic peak and its intensity attenuates rapidly due to surface roughness. Note also that the full width at half maxima (FWHM) of  $9.8 \text{ meV}$  for the  $1048 \text{ cm}^{-1}$  phonon feature is only slightly larger than  $9.7 \text{ meV}$  found for the elastic peak for the monolayer structure [Fig. 2(a)], consistent with the  $1048 \text{ cm}^{-1}$  phonon feature arising from a single phonon excitation.<sup>27</sup>

From the above discussion of the possible arrangements of  $[\text{SiO}_4]$  tetrahedra on the Mo(112) surface [Figs. 4 and 5(a)], at least one and possibly two Si-O species<sup>28</sup> are formed, specifically a Si-O-Mo and/or a Si-O-Si species. A Si-O-Mo asymmetric stretching mode has been reported at approximately  $930 \text{ cm}^{-1}$ ,<sup>30,31</sup> as shown in Table I. Based on previous Si-O-Si and Si-O-Ti assignments of IR<sup>29,32–34</sup> and HREELS<sup>22–24,35</sup> data, the  $1048 \text{ cm}^{-1}$  phonon feature likely corresponds to the Si-O-Mo asymmetric stretching mode. The differences between the HREELS and IRS data might

well be explained using the rational applied to similar data for  $\text{Al}_2\text{O}_3$ .<sup>38</sup>

That the film thickness and/or influence of the Mo substrate could shift the Si-O-Si asymmetric stretching phonon from  $1176$  to  $1048 \text{ cm}^{-1}$  has been considered since oxide film thickness<sup>39–41</sup> and metals<sup>42–44</sup> have been reported to effect phonon features by  $30$ – $40 \text{ cm}^{-1}$ . The present redshift of  $128 \text{ cm}^{-1}$ , however, is far too large to be attributed exclusively to effects of substrate coupling or to thinness of the film. Furthermore, the  $1048 \text{ cm}^{-1}$  phonon peak position is independent of the  $\text{SiO}_2$  coverage (Fig. 3), consistent with excluding a significant influence of substrate coupling on the phonon redshift.

Because the film is one monolayer thick, it is inevitable that the  $[\text{SiO}_4]$  tetrahedra share one or more of their four oxygen atoms with the substrate Mo atoms, i.e., Si-O-Mo bonds (see Figs. 4 and 5). It follows from their bonding geometry [Fig. 5(a)], these Si-O-Mo species should have rather large, asymmetric stretching dipole components perpendicular to the surface. Therefore, it is reasonable to assign the single phonon excitation peak at  $1048 \text{ cm}^{-1}$  to the asymmetric stretching of the Si-O-Mo species. That coupling effects from the Mo substrate metal surface could shift the

TABLE I. Observed IR and HREELS frequencies of different Si-O-X asymmetric stretching modes

Si-O species	IR frequency ( $\text{cm}^{-1}$ )	HREELS ( $\text{cm}^{-1}$ )
Si-O-Si ( $\text{SiO}_2$ )	1070–1100 (Refs. 29 and 32)	1176 (Refs. 22–24, present)
Si-O-Si ( $\text{SiO}_x$ )	980–1080 (Ref. 33)	1050–1150 (Refs. 23 and 24)
Si-O-Ti	935–960 (Ref. 34)	1025–1040 (Ref. 35)
Si-O-Mo	$\sim 930$ (Refs. 30 and 31)	1048 (present)
Si-O-Al	$\sim 1000$ (Ref. 29)	
Si-O-Zr	950 (Ref. 36)	
Si-O-Ln	$\sim 900$ (Ref. 37)	

phonon peak of Si-O-Si asymmetric stretching from 1176 to 1048  $\text{cm}^{-1}$  can also be ruled out because the infrared vibrational frequencies for the two species Si-O-Mo and Si-O-Si of 930 and 1070  $\text{cm}^{-1}$ , respectively (see Table I), should likewise be similarly shifted, which is not the case.

From the above discussion, it is apparent that no phonon features (near 1176 and 500  $\text{cm}^{-1}$ , corresponding to asymmetric stretching and bending modes, respectively) in the HREEL spectra arise from a Si-O-Si species in a single layer  $\text{SiO}_2/\text{Mo}(112)$  structure. In order that there be a Si-O-Si species on the surface with no component perpendicular to the surface, the three atoms in the Si-O-Si linkage must be arranged such that the plane of the Si-O-Si species is parallel to the surface. Referring to the structural models of Fig. 4 and Fig. 5(a), models 2–8 all have Si-O-Si linkages with angles between 108 and 135°, with their planes tilted or perpendicular to the surface plane. Such species should exhibit phonon features near 496 and 1176  $\text{cm}^{-1}$ , therefore, models 2–8 can be ruled out. Although the Si-O-Si species in these models could be forced to have their plane parallel to the surface, such a configuration would be energetically unfavorable.

From the above discussion, model 1 appears to be the only possible structure of the  $[\text{SiO}_4]$  network that will yield the observed HREEL spectra. The coordination of this geometry to the  $\text{Mo}(112)$  surface is shown in Fig. 5(b) and is characterized as  $\text{Mo}(112)\text{-}c(2\times 2)\text{-}[\text{SiO}_4]$ . In the proposed structural model, each Si atom is bonded with four oxygen atoms to form a tetrahedron located at a trough on the  $\text{Mo}(112)$  surface. In this structure, the two oxygen atoms in the trough bind with the second and/or the first layer Mo atoms like threefold hollow or bridging sites, and two oxygen atoms at the outermost surface bind with the first layer Mo atoms in bridging or atop sites. In the actual structure, the Mo substrate surface must also restructure to best accommodate the  $[\text{SiO}_4]$  tetrahedra on the surface, and the  $[\text{SiO}_4]$  unit might also rotate to achieve the optimum coordination geometry. There very well may be an additional oxygen atom

located among the four  $[\text{SiO}_4]$  units and bonded only to the substrate Mo since a phonon feature is observed at 672  $\text{cm}^{-1}$ , a value very near that found for a O-Mo(112) surface.

That each  $[\text{SiO}_4]$  tetrahedron in the proposed model has four exceptionally strong Si-O-Mo bridge bonds to the substrate Mo can explain why the monolayer structure is stable upon annealing at 1250 K in UHV. Thicker films (between 1 and 3 ML), on the other hand, slowly decompose and form the monolayer structure at this annealing temperature even in  $5\times 10^{-6}$  Torr  $\text{O}_2$ . The monolayer structure is also extremely unreactive as evidenced by the fact that no carbon contamination or water adsorption was observed under vacuum condition of  $5\times 10^{-10}$  Torr for several days. Even after exposure to atmospheric conditions, a clean monolayer structure can be regenerated by annealing to 1000 K in vacuum.

## V. CONCLUSIONS

Thin  $\text{SiO}_2$  films on  $\text{Mo}(112)$  have been prepared and characterized. A well ordered monolayer  $\text{Mo}(112)\text{-}c(2\times 2)\text{-}[\text{SiO}_4]$  structure was found that shows unique HREELS phonon features compared to thick  $\text{SiO}_2$  films or to bulk  $\text{SiO}_2$ . The unique phonon peak at 1048  $\text{cm}^{-1}$  was assigned to be asymmetric stretching of a Si-O-Mo species. A structural model was derived where all four oxygen atoms in a  $[\text{SiO}_4]$  tetrahedron bond to the substrate Mo atoms, i.e., no Si-O-Si bridge bonds are present on the surface. This monolayer  $\text{Mo}(112)\text{-}c(2\times 2)\text{-}[\text{SiO}_4]$  structure is stable and highly reproducible.

## ACKNOWLEDGMENTS

We acknowledge with pleasure the support of this work by the Department of Energy, Office of Basic Energy Sciences, Division of Chemical Sciences, the Robert A. Welch Foundation and the Texas Advanced Technology Program under Grant No. 010366-0022-2001.

\*Author to whom correspondence should be addressed. Electronic address: goodman@mail.chem.tamu.edu

<sup>1</sup>H. J. Freund, *Surf. Sci.* **500**, 271 (2002).

<sup>2</sup>C. R. Henry, *Surf. Sci. Rep.* **31**, 235 (1998).

<sup>3</sup>C. T. Campbell, *Surf. Sci. Rep.* **27**, 1 (1997).

<sup>4</sup>D. W. Goodman, *Surf. Rev. Lett.* **2**, 9 (1995).

<sup>5</sup>J. Albert, *Introduction of Glass Integrated Optics*, edited by S. I. Najafi (Artech House, Boston, 1992).

<sup>6</sup>A. Laschitsch and D. Johannsmann, *J. Appl. Phys.* **85**, 3759 (1999).

<sup>7</sup>L. Spassov and D. Y. Yonkov, *Rev. Sci. Instrum.* **65**, 721 (1994).

<sup>8</sup>G. S. Siu, X. L. Wu, and X. M. Bao, *Appl. Phys. Lett.* **74**, 1812 (1999).

<sup>9</sup>Z. Liu, H. Li, X. Feng, S. Ren, and H. Wang, *J. Appl. Phys.* **84**, 1913 (1998).

<sup>10</sup>T. Schroeder, M. Aldelt, B. Richter, M. Naschitzki, M. Baumer, and H.-J. Freund, *Surf. Rev. Lett.* **7**, 7 (2000).

<sup>11</sup>T. Schroeder, J. B. Giorgi, M. Baumer, and H.-J. Freund, *Phys. Rev. B* **66**, 165422 (2002).

<sup>12</sup>M. Kundu and Y. Murata, *Appl. Phys. Lett.* **80**, 1921 (2002).

<sup>13</sup>A. K. Santra, B. K. Min, and D. W. Goodman (unpublished).

<sup>14</sup>Y. D. Kim, T. Wei, and D. W. Goodman, *Langmuir* **19**, 354 (2003).

<sup>15</sup>S. Wendt, Y. D. Kim, and D. W. Goodman, *Prog. Surf. Sci.* **74**, 141 (2003).

<sup>16</sup>A. K. Santra, B. K. Min, and D. W. Goodman, *Surf. Sci.* **515**, L475 (2002).

<sup>17</sup>B. K. Min, A. K. Santra, and D. W. Goodman, *J. Vac. Sci. Technol. B* **21**, 2319 (2003).

<sup>18</sup>Y. D. Kim, T. Wei, S. Wendt, and D. W. Goodman, *Langmuir* **19**, 7929 (2003).

<sup>19</sup>E. Ozensoy, B. K. Min, A. K. Santra, and D. W. Goodman, *J. Phys. Chem. B* (in press).

<sup>20</sup>H. H. Madden and D. W. Goodman, *Surf. Sci.* **150**, 39 (1985).

<sup>21</sup>S. Tanuma, C. J. Powell, and D. R. Penn, *Surf. Interface Anal.* **17**, 911 (1991).

<sup>22</sup>P. A. Thiry, M. Liehr, J. J. Pireaux, R. Sporken, R. Caudano, J. P. Vigneron, and A. A. Lucas, *J. Vac. Sci. Technol. B* **3**, 1118



- (1985).
- <sup>23</sup>J. A. Schaefer and W. Gopel, *Surf. Sci.* **155**, 535 (1985).
- <sup>24</sup>H. Ibach, H. D. Bruchmann, and H. Wagner, *Appl. Phys. A: Solids Surf.* **29**, 113 (1982).
- <sup>25</sup>D. A. Keen and M. T. Dove, *J. Phys.: Condens. Matter* **11**, 9263 (1999).
- <sup>26</sup>N. H. de Leeuw, F. M. Higgins, and S. C. Parker, *J. Phys. Chem. B* **103**, 1270 (1999).
- <sup>27</sup>A. A. Lucas, and M. Sunjie, *Prog. Surf. Sci.* **2**, 75 (1972).
- <sup>28</sup>Both vitreous and crystalline SiO<sub>2</sub> consist of continuous [SiO<sub>4</sub>] tetrahedral network by sharing vertex oxygens forming [Si-O-Si] bridges. Thus, their vibrational spectra can be interpreted in terms of a [SiO<sub>4</sub>] [E. Dowty, *Phys. Chem. Miner.* **14**, 122 (1987)] or a [Si-O-Si] [R. J. Bell and P. Dean, *Disc. Faraday Soc.* **50**, 55 (1970)] unit, the latter being more physically realistic. For example, in potassium alumino-silicates (K<sub>2</sub>O-Al<sub>2</sub>O<sub>3</sub>-SiO<sub>2</sub>) whose networks consist of linked [AlO<sub>4</sub>] and [SiO<sub>4</sub>] tetrahedra, two Si-O asymmetric stretching modes at approximately 1100 and 1000 cm<sup>-1</sup>, corresponding to [Si-O-Si] and [Si-O-Al] linkages, respectively, are observed (Ref. 29).
- <sup>29</sup>M. Handke and W. Mozgawa, *Vib. Spectrosc.* **5**, 75 (1993).
- <sup>30</sup>S. R. Seyedmonir, S. Abdo, and R. F. Howe, *J. Phys. Chem.* **86**, 1233 (1982).
- <sup>31</sup>M. Cornac, A. Janin, and J. C. Lavalley, *Polyhedron* **5**, 183 (1986); *Infrared Phys.* **24**, 143 (1984).
- <sup>32</sup>J. F. Scott and S. P. S. Porto, *Phys. Rev.* **161**, 903 (1967).
- <sup>33</sup>M. Nakamura, Y. Mochizuki, K. Usami, Y. Itoh, and T. Nozaki, *Solid State Commun.* **50**, 1079 (1984).
- <sup>34</sup>Z. F. Liu and R. J. Davis, *J. Phys. Chem.* **98**, 1253 (1994).
- <sup>35</sup>M. S. Chen and D. W. Goodman (unpublished).
- <sup>36</sup>G. Lucovsky and G. B. Rayner, *Appl. Phys. Lett.* **77**, 2912 (2000).
- <sup>37</sup>H. Ono, *Appl. Phys. Lett.* **78**, 1832 (2001).
- <sup>38</sup>M. Liehr, P. A. Thiry, J. J. Pireaux, and R. Caudano, *J. Vac. Sci. Technol. A* **2**, 1079 (1984).
- <sup>39</sup>K. T. Queeney, M. K. Weldon, J. P. Chang, Y. J. Chabal, A. B. Gurevich, J. Sapjeta, and R. L. Opila, *J. Appl. Phys.* **87**, 1322 (2000).
- <sup>40</sup>P. Bruesch, R. Kotz, H. Neff, and L. Pietronero, *Phys. Rev. B* **29**, 4691 (1984).
- <sup>41</sup>C. Martinel and P. A. B. Devine, *J. Appl. Phys.* **77**, 4343 (1995).
- <sup>42</sup>M. Wada and N. Tanaka, *Jpn. J. Appl. Phys.* **29**, L1497 (1990).
- <sup>43</sup>N. Tanaka, *J. Mater. Sci. Technol.* **13**, 265 (1997).
- <sup>44</sup>E. Wackelgard, *J. Phys.: Condens. Matter* **8**, 5125 (1996).